Published online February 27, 2004

1404–1413 *Nucleic Acids Research, 2004, Vol. 32, No. 4*
DOI: 10.1093/nar/gkh318

Two-hybrid Mpp10p interaction-defective Imp4 proteins are not interaction defective *in vivo* but do confer specific pre-rRNA processing defects in *Saccharomyces cerevisiae*

Jennifer E. G. Gallagher[1] and Susan J. Baserga[1,2,3,*]

[1]Department of Genetics, [2]Department of Molecular Biophysics and Biochemistry and [3]Department of Therapeutic Radiology, Yale University School of Medicine, New Haven, CT 06520-8024, USA

Received January 26, 2004; Revised and Accepted February 6, 2004

ABSTRACT

The SSU processome is a large, evolutionarily conserved ribonucleoprotein (RNP), consisting of the U3 snoRNA and at least 28 protein components, that is required for biogenesis of the 18S rRNA. We tested the function of one protein–protein interaction in the SSU processome, Mpp10p–Imp4p, in ribosome biogenesis. Exploiting the reverse two-hybrid system, we screened for mutated Imp4 proteins that were conditionally defective for interaction with Mpp10p. Three different *imp4* sequences were isolated that: (i) conferred conditional growth in the two-hybrid strain; (ii) complemented the disrupted *imp4*; (iii) conferred conditional growth in the context of their normal cellular function; and (iv) resulted in defective pre-rRNA processing at the non-permissive temperatures. Domain swapping revealed that mutations that conferred cold sensitivity resided in the N-terminal coiled-coil domain while mutations in the C-terminus conferred temperature sensitivity. Surprisingly, the mutated Imp4 proteins were not measurably defective for interaction with Mpp10p in the context of the SSU processome. This suggests that other members of the complex may contribute to maintaining the Mpp10p–Imp4p interaction in this large RNP. Since protein–protein interactions are critical for many different aspects of cellular metabolism, our work has implications for the study of other large protein complexes.

INTRODUCTION

In eukaryotes, ribosome biogenesis requires the coordination of many different events, including rRNA transcription, pre-rRNA modification and processing, ribosomal protein production and rRNA–ribosomal protein assembly. Pre-rRNA modification occurs early in ribosome biogenesis on the RNA polymerase I-transcribed nascent pre-rRNA (1). In *Saccharomyces cerevisiae* this 35S rRNA bears three rRNAs (18S, 5.8S and 25S), which are subsequently released from their nascent transcripts by pre-rRNA cleavages (Fig. 1). The U3 snoRNA and its associated proteins form a large ribonucleoprotein (RNP), the SSU processome, which is required for the three cleavage events that mature the 18S rRNA (A0, A1 and A2) (3). The SSU processome is associated with the 35S and 23S pre-rRNAs, both of which retain the U3-dependent cleavage sites (4). U3 snoRNA–pre-rRNA base pairing is required for cleavage, and this likely occurs in the context of the SSU processome (5,6).

Mpp10p, Imp4p and Imp3p are three protein components of the SSU processome that are essential for its function. Mpp10p was originally discovered in a screen for human proteins that are phosphorylated during mitosis (7). Mpp10p in both humans and yeast is specifically associated with the U3 snoRNA, and is required for pre-rRNA processing (8,9). Mpp10p bears multiple protein–protein interaction domains (coiled-coil) and indeed has been found to interact with two proteins in a two-hybrid screen and *in vivo*, Imp3p and Imp4p (10). We have hypothesized that Imp3p contacts the U3 snoRNA directly via its ribosomal protein S4 RNA binding motif. Imp4 is the founding member of the Imp4 superfamily, and as such bears the σ^{70}-like RNA binding motif (4). Like Mpp10p, both Imp3p and Imp4p are U3 snoRNA-associated and are required for pre-rRNA processing (10).

In a large RNP with 28+ proteins like the SSU processome, it is likely that multiple protein–protein interactions occur and that they are essential for SSU processome function. We tested the role of one of these protein–protein interactions, Mpp10p–Imp4p, in ribosome biogenesis. We used the reverse two-hybrid system approach to create conditionally Mpp10p interaction-defective mutated Imp4ps. Because an essential gene encodes Imp4p, we screened for the subset of Mpp10p interaction-defective mutated Imp4ps that also conferred growth at the permissive temperature. Three different mutated Imp4ps were obtained that were interaction defective in the two-hybrid screen and conferred growth at the permissive but not at the non-permissive temperatures. Surprisingly, when tested by co-immunoprecipitation, Mpp10p–Imp4p

*To whom correspondence should be addressed at Yale University School of Medicine, Department of Molecular Biophysics and Biochemistry, 333 Cedar Street, PO Box 208024, New Haven, CT 06530-8024, USA. Tel: +1 203 785 4618; Fax: +1 203 785 6404; Email: susan.baserga@yale.edu

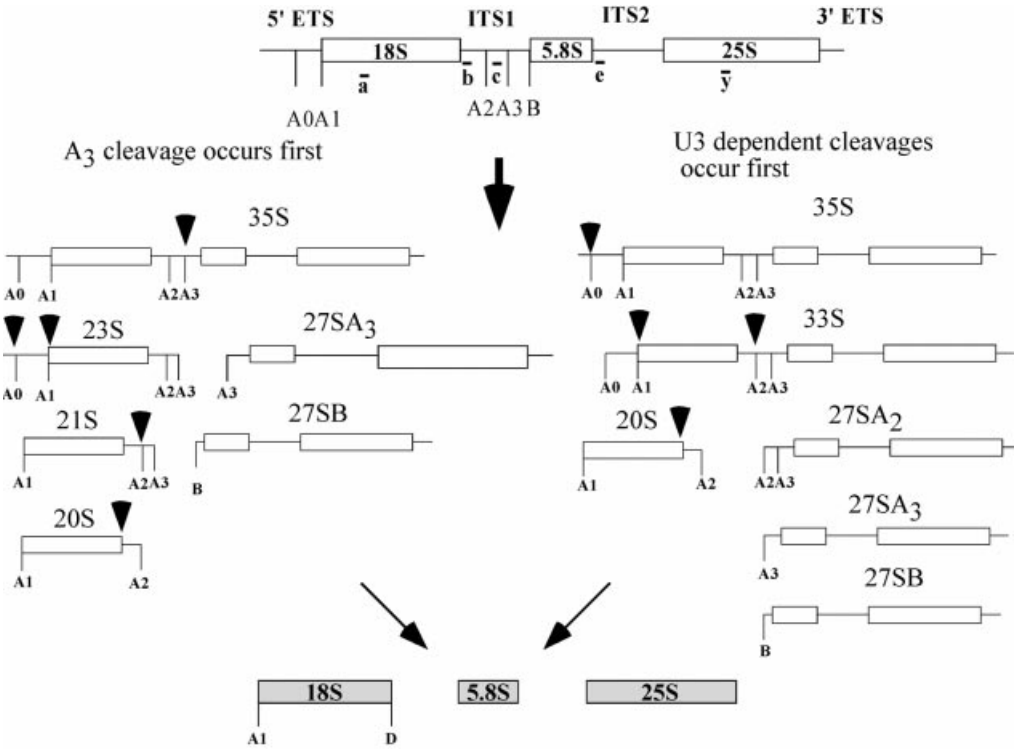

Figure 1. Steps in pre-rRNA processing in *Saccharomyces cerevisiae*. The precursors to the 18S rRNA mature along two different processing pathways depending on which cleavage event in ITS1 occurs first. Cleavage can occur at the SSU processome-dependent cleavage at A_2 or the RNase MRP-dependent cleavage at A_3. Either cleavage separates the rRNAs destined for the large ribosomal subunit (5.8S and 25S) from the one destined for the small ribosomal subunit (18S). Both sides of the pathway lead to production of identical 18S rRNAs. ETS, external transcribed spacer; ITS, internal transcribed spacer.

interaction was not compromised at the non-permissive temperatures in the context of the SSU processome. However, pre-rRNA processing was defective at the non-permissive temperatures, indicating a function for particular domains of Imp4p in specific pre-rRNA cleavage steps.

MATERIALS AND METHODS

Plasmids, strains and antibodies

To map the interacting portions of Mpp10p with Imp4p, *MPP10* and truncations of *MPP10* were cloned into the plasmid encoding the *GAL4* DNA binding domain (bait), pAS2-1. *IMP4* was cloned into the plasmid with the *GAL4* activation domain (prey), pACT-2. Strain MaV103 was used for the two-hybrid analysis (11). To map the interacting portions of Imp4p with Mpp10p, *IMP4* and truncations of *IMP4* were cloned into pAS2-1, and *MPP10* was cloned into pACT-2. Strain pJ69-4A was used for the two-hybrid analysis (12). For the reverse two-hybrid screen, pAS2-1-*imp4* was mutagenized and screened for interaction with the product of pACT-2-*MPP10.* Strain pJ69-4A was used for the screen. JA300, a tryptophan auxotropic *Escherichia coli* strain, was used to recover pAS2-1-*imp4* plasmids (13). The *imp4* alleles were expressed from the yeast constitutive plasmid p415GPD *imp4* and shuffled into the *pGAL1::IMP4* (YPH259 Δ*imp4::HIS3*) yeast strain.

Polyclonal antibodies were raised against Imp4p purified from *E.coli* expressed from the pET28 vector using the TALON kit (Clontech). At least 250 μg of purified protein was injected monthly into guinea pigs and sera were tested for reactivity starting 3 months after the first injection by western blots on purified Imp4p and whole cell lysates. Anti-Mpp10p rabbit polyclonal antibodies were previously described (9). Anti-HA monoclonal antibodies were prepared from hybridoma cell line 12CA5.

Mapping Mpp10p–Imp4p interacting domains

pAS2-1-*MPP10* (bait) was previously described (10) and consists of *MPP10* encoding amino acids 1–498 fused to the *GAL4* DNA binding domain. *MPP10* truncations representing amino acids 1–450, 1–400, 1–350, 1–300, 350–593 and 400–593 were generated using the polymerase chain reaction (PCR) with the appropriate oligonucleotides bearing XhoI and XmaI restriction sites. The gel-purified PCR products were cut with XhoI and XmaI and cloned into pAS2-1 cut with SalI and XmaI. In-frame fusion with the *GAL4* binding domain was verified by automated DNA sequencing. Plasmids encoding Mpp10p truncations were transformed into the MaV103 strain harboring the *IMP4* prey plasmid (pACT-2-*IMP4*), and transformants with both plasmids were selected on SD-Trp, Leu. Colonies were patched in duplicate onto SD-Trp, Leu plates and beta-galactosidase activity was assayed as previously described (10).

Two truncations of Imp4p were analyzed for interactions with Mpp10p in the two-hybrid assay. They represent amino acids 50 to the C-terminus and the N-terminus to 50. The first construct (amino acids 50 to end) was generated by PCR with the appropriate oligonucleotides bearing XhoI and XmaI

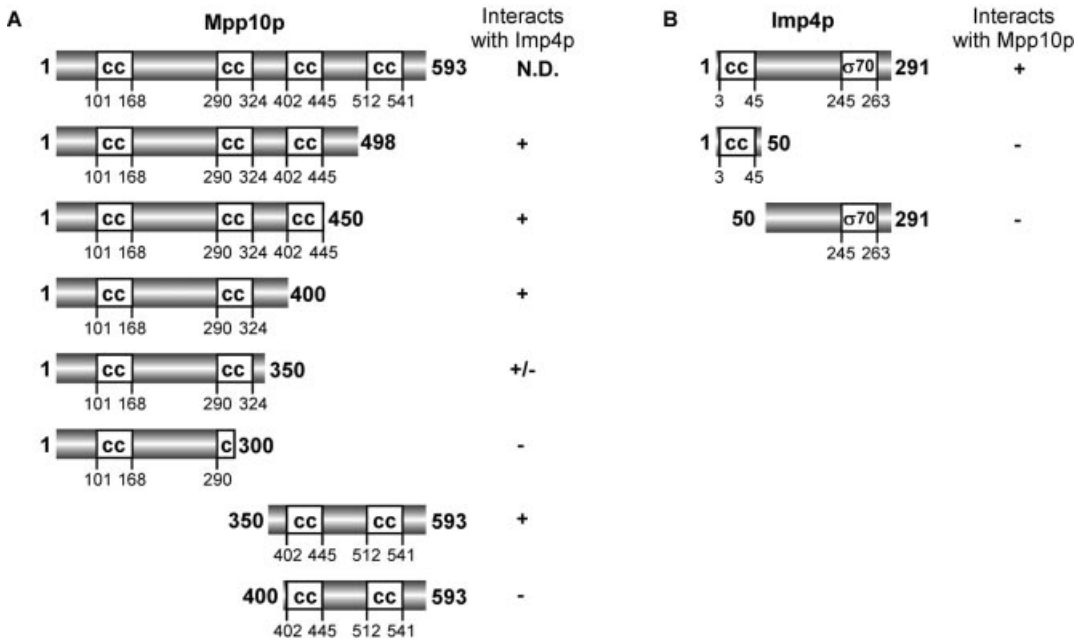

Figure 2. Mapping protein sequences required for Mpp10p–Imp4p interaction. (**A**) Mpp10p sequences required for Imp4p interaction. The coiled-coil (cc) domains of Mpp10 predicted by the COILS program are indicated. N- and C-terminal truncations of Mpp10p were tested for their interaction with Imp4p using the two-hybrid system. The + sign indicates dark blue, the +/– sign light blue and the – sign white in the beta galactosidase assay. (**B**) Imp4p sequences required for Mpp10p interaction. The cc domain predicted by the COILS program is indicated. Two Imp4p truncations were tested for interaction with Mpp10p using the two-hybrid system. The + sign indicates growth on SD-Leu, Trp, His while the – sign indicates no growth.

restriction sites, cut with these enzymes and then cloned into SalI and XmaI-cut pAS2-1. The second construct (amino acids 1–50) was generated by PCR with the appropriate oligonucleotides bearing NcoI and BamHI restriction sites and then cloned into pAS2-1 cut with the same enzymes. Both were subject to automated sequencing to verify in-frame fusion. Plasmids encoding Imp4p truncations were transformed into pJ69-4A bearing pACT-2-*MPP10*, selected on SD-Trp, Leu plates and tested for interaction by serial dilution on SD-Trp, Leu, His plates.

Mutagenic PCR

To create a two-hybrid bait plasmid with the *IMP4* gene for mutagenic PCR, the *GAL4* DNA binding domain of pAS2-1 was fused in-frame to the N-terminus of *IMP4*. *IMP4* was amplified from the plasmid template pGAD3::*IMP4* using PCR amplification with primers that contained 30 nt (capitalized) of the vector extending outwards from the cloning site (underlined). The 5′ primer sequence also contained the NcoI restriction site and 15 nt (lower case) of the *IMP4* coding sequence; BDIMP4-1 (5′-TAC CCA GCT TTG ACT CAT ATG GCC ATG GAG atg cta aga aga caa-3′). The 3′ primer BDIMP4-2 sequence is 5′-aaa ttc gcc cgg att TAG CTT GGC TGC AGG TCA CAA ATA GTC TTT-3′ and contains a PstI restriction site. Mutagenic PCR was carried out using reduced dNTP levels, $MnCl_2$ and an excess of *Taq* polymerase. The reaction conditions for the mutagenic PCR were: 1× Promega PCR buffer, 4.5 mM $MgCl_2$, 4.95 mM $MnCl_2$, 0.5 mM dTTP, 0.5 mM dCTP, 0.1 mM dATP, 0.1 mM dGTP, 2 ng of pGAD3::*IMP4* template, 4 ng of each BDIMP4 primer and 5 units of *Taq* DNA polymerase (Roche) per 100 µl reaction. The PCR conditions were as follows: 94°C for 5 min and then 30 cycles of 94°C for 1 min, 55°C for 2 min and 72°C for 3 min, and then 72°C for 20 min to finish.

Screen for Imp4p proteins that are conditionally defective for interaction with Mpp10p

We used the two-hybrid system to screen for Mpp10p interaction-defective Imp4 proteins (Fig. 3). To create the necessary strain, pJ69-4A cells were transformed with the *MPP10* plasmid cloned into pACT-2 (prey) (10). The PCR products of 10 mutagenic reactions were gel purified and co-transformed with 25 µg of NcoI/PstI linearized pAS2-1plasmid (bait) into 12 ml of cells grown to 0.5 OD_{600}. Because the mutagenic PCR product contains sequence homology to the gapped vector, it serves as a substrate for homologous recombination via DNA repair pathways (gapped-repair transformation) (14), creating a library of mutated *imp4* alleles. Transformants of the two-hybrid strain were grown at 30°C and selected on SD-Leu, Trp, His media, which selected for the *GAL* activating–*MPP10* fusion plasmid (-Leu), the library of *imp4* mutations with the *GAL* DNA binding plasmid (-Trp) and activation of the histidine reporter gene. Transformants that could grow on this selective medium have repaired the gapped pAS2-1 plasmid with the PCR-mutagenized *imp4* gene. Also, to grow in SD-His medium at 30°C, the transformants must also have mutagenized *imp4* fusions proteins interacting with the Mpp10 fusion protein, thereby activating the histidine reporter gene. To screen for Imp4 proteins conditionally defective for Mpp10p interaction at 17 and 37°C, colonies were picked and their growth tested. Colonies that grew on SD-His at 30°C but not at 17 or 37°C were considered to be candidates for possessing an interaction-defective mutated Imp4p. The pAS2-1 *imp4* plasmids

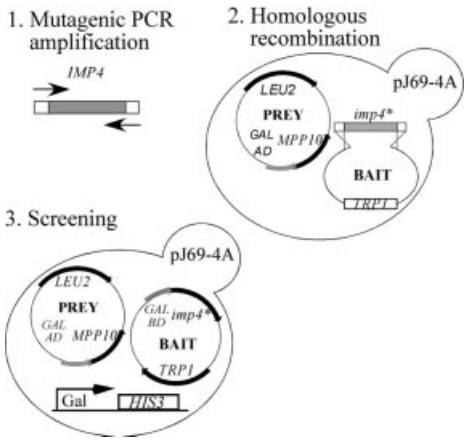

Figure 3. Strategy for creating Imp4 proteins which are conditionally defective for interaction with Mpp10p. (1) *IMP4* sequences with flanking sequences homologous to the two-hybrid system bait plasmid were amplified by mutagenic PCR. (2) The PCR product was co-transformed with the gapped bait plasmid into a strain (pJ69-4A) that harbored *MPP10* cloned into the two-hybrid system prey plasmid. The bait plasmid containing mutagenized *IMP4* was thus constructed by gap repair. (3) If the proteins encoded by the bait and prey plasmids interact, the *GAL* promoter is activated and the *HIS* gene is expressed. To screen for Imp4 proteins that are conditionally defective for Mpp10p interaction, yeast were screened for *HIS* expression at 30°C (permissive) and 17 and 37°C (non-permissive). Bait plasmids from yeast that grew at the permissive but neither of the non-permissive temperatures were rescued and studied further (Table 1).

from these colonies were recovered by electroporation of total yeast DNA isolated by HIRT lysates of these strains into an *E.coli* strain auxotropic for tryptophan, JA300. On M9 media lacking tryptophan, only transformants with the pAS2-1 plasmid grow. These colonies were then replica plated on carbenicillin plates to eliminate false positives. The pAS2-1-*imp4* plasmids recovered from *E.coli* were transformed back into the starting strain (pJ69-4A containing pACT-2-*MPP10*) and re-screened to confirm the plasmid dependence of the observed conditional growth.

Complementation of Δ*imp4* (null allele) by mutated *imp4* alleles

To determine whether the candidate interaction-defective Imp4 proteins maintained their conditional growth defect outside the context of the two-hybrid system, the following tests were performed. Because *IMP4* is an essential gene, the mutated Imp4 proteins were tested for their ability to support growth. The pAS2-1-*imp4* plasmids recovered above were amplified by PCR with 5′ pAS2-1.SpeI primer (5′-GCT TTG ACT AGT ATG GCC ATG GAG-3′) and 3′ pAS2-1.PstI primer (5′-CGG AAT TAG CTT GGC TGC AGG-3′). These primers anneal to the vector sequence, amplifying only the *imp4* coding region. Using the designated restriction sites, the mutated *imp4* genes were cloned into p415GPD, a constitutive expression vector with *LEU2* marker (15). The plasmids were transformed into the *pGAL1::IMP4* (Δ*imp4::HIS3*) strain carrying a wild-type copy of *IMP4* on pGAD3, a *URA3* plasmid (10). The pGAD3 plasmid was shuffled out on 5-FOA, which selects against the uracil prototrophs. The strains were re-grown on SC-Leu and SC-Ura plates to confirm the presence of only the p415GPD plasmid. Strains that did not grow after plasmid shuffling were interpreted as bearing a non-complementing *imp4* allele. Colonies that grew on SD-Leu, Trp, His at 30°C but not at 17 or 37°C were selected for further study. The results of each step of the screening procedure are summarized in Table 1. Candidate Mpp10p interaction-defective *imp4* genes were sequenced by the Keck facility at Yale University School of Medicine (Fig. 4).

Analysis of Mpp10p–Imp4p interaction and SSU processome integrity

Co-immunoprecipitation of Imp4p and Mpp10p was analyzed in extracts made from 10 ml of cells grown to 0.5 OD_{600}. Proteins were extracted by vortexing with glass beads in 600 µl of NET-2 (150 mM NaCl, 0.01% NP-40, 20 mM Tris–HCl pH 7.5) and 4.2 µl of 150× protease inhibitor cocktail (Roche). Imp4p antibodies were bound to 2.5 mg of protein A–Sepharose CL-4B beads (Pharmacia) by incubation with 10 µl of guinea pig sera and 500 µl of NET-2 overnight at 4°C on a nutator. Immunoprecipitations were performed in antibody excess, as determined by titration. Beads were washed three times with NET-2 to remove unbound antibody, and were incubated with 500 µl of lysate for 1 h at 4°C on a nutator. The beads were then washed seven times with NET-2 and resuspended in 5 µl of 5× SDS loading dye and boiled for 3 min at 95°C. Total protein from each lysate was also included, and represented 5% of the total amount in each immunoprecipitation. Proteins were separated on a 10% SDS–PAGE gel, transferred to Immobilon™-P and incubated with 1:10 000 dilution of anti-Mpp10p antibody (9) for 1 h at room temperature. Anti-mouse secondary antibody conjugated to HRP diluted 1:10 000 was then added for 15 min. Immunoreactive bands were visualized with ECL™ from Amersham Pharmacia Biotech according to the manufacturer's instructions. Bands were quantitated on an Alpha Innotech imager.

Co-immunoprecipitations with Nop1p-HA were carried out with extract prepared from strains each carrying alleles of *imp4*. Nop1p was tagged chromosomally at the C-terminus with a triple HA tag (16). For anti-HA immunoprecipitations 200 µl of 12CA5 was bound to 2.5 µg of protein A Sepharose beads for 1 h at room temperature. The co-immunoprecipitations were then carried out as described for anti-Imp4p co-immunoprecipitations. Western blots of co-immunoprecipitations were blotted with 1:500 dilution of 12CA5 for 1 h at room temperature and then 1:10 000 dilution of anti-mouse secondary antibody conjugated to HRP to detect HA tagged Nop1p.

Domain swapping of mutated Imp4ps

In order to narrow down which mutations in *imp4* caused which conditional growth phenotypes, domains of the mutated alleles were swapped with domains from the wild-type *IMP4* gene and cloned into p415GPD. The 5′ region domain, which encodes the coiled-coil region, extended from the start codon to the BamHI site at nucleotide 243; the 3′ domain extended from the BamHI site to the stop codon (Fig. 6). Conditional growth of yeast was tested by transforming the *pGAL1::IMP4* strain with p415GPD *imp4* plasmids, followed by plasmid shuffle (10). For quantitative analysis, serial dilution of strains grown at 30, 17 and 37°C was carried out on SD-Leu plates.

Table 1. Numerical tabulation of the results from the two-hybrid screen for mutated Imp4 proteins that are defective for interaction with Mpp10p

imp4 alleles	Two-hybrid strain pJ69-4A Conditional growth	After rescue	YPH259 Δ*imp4* Δ*imp4* complementation	Conditional growth
imp4-1	ts	ts	–	
imp4-2	ts	ts	+	ts
imp4-3	ts	ts	+	cs/ts
imp4-4	ts	ts	+	X
imp4-5	cs	cs	+	ND
imp4-6	ts	ts	+	X
imp4-7	cs	X		
imp4-8	cs	X		
imp4-9	ts	X		
imp4-10	ts	ts	+	X
imp4-11	ts	ts	+	cs/ts
imp4-12	ts	ts	+	ts
imp4-13	cs	cs/ts	–	
imp4-14	cs	cs	–	
imp4-15	cs	cs	–	
imp4-16	cs	X		
imp4-17	ts	ts	+	ts
imp4-18	ts	X		
imp4-19	ts	X		
ts	11	9	8	3
cs	8	3	0	0
cs/ts	0	1	0	2
Total	19	13	8	5

Nineteen colonies were isolated that were either cold (17°C) or temperature (37°C) sensitive for growth in medium lacking histidine. Subsequent rescue of each *imp4* bait plasmid and re-transformation into the pJ69-4A strain bearing the *MPP10* prey plasmid reduced the number to 13. The *imp4* inserts were cloned into the yeast expression vector p415GPD and assessed for their ability to confer growth to a strain where the *IMP4* gene has been disrupted. There were eight plasmids that could complement the Δ*imp4* strain; of these, five conferred conditional growth at either 17 or 37°C and were studied further.

RNA analysis

All strains were grown at 30°C until early log phase and then shifted to 37 or 17°C as indicated. Aliquots were collected 0, 3, 6 and 9 h after the shift while keeping the OD_{600} of each culture below 0.5. Total RNA was harvested from 20 ml of cells at 0.5 OD_{600} using the hot phenol method (17). To analyze pre-rRNA, 10 μg of RNA was run on a 20 × 25 cm, 1.25% agarose–formaldehyde gel for 24 h at 59 V with recirculated buffer. The RNA was transferred overnight to Genomic GT Zeta probe membrane. To analyze small RNAs, 10 μg of total RNA was separated on an 8% polyacrylamide gel and transferred by Bio-Rad semi-dry transfer apparatus at 24 V, 300 mA and 3 W for 45 min. Hybridizations of northern blots were done with [γ-^{32}P]ATP-labeled oligonucleotides complementary pre-rRNA, rRNA and U3 snoRNA, as previously described (9). Oligos a, b, c and e were described in Beltrame and Tollervey (18) and oligo y was described in Samarsky and Fournier (19). Primer extensions were carried out as described in Maden *et al.* (20).

RESULTS

Imp4p was originally identified as an Mpp10p-interacting protein in a two-hybrid screen. To pinpoint the interacting domains of Mpp10p with Imp4p and of Imp4p with Mpp10p, a series of truncations of each were generated and tested with the other in the two-hybrid assay.

The Mpp10 protein possesses a number of coiled-coil domains (Fig. 2A), known to be protein–protein interaction domains, and it was likely that one such domain would be required for interaction with Imp4p. The original two-hybrid screen with Mpp10p, which identified Imp3p and Imp4p as interacting proteins, was carried out with an Mpp10p truncated at its C-terminus (amino acids 1–498), thus missing one coiled-coil domain, because the full-length Mpp10p autoactivated in the beta galactosidase assay (10). A series of Mpp10p truncations was made from both the N- and C-termini, and tested for interaction with Imp4p in the two-hybrid assay (Fig. 2A). Truncations from the C-terminus indicated that the Mpp10p fragment of only amino acids 1–350 began to display reduced Imp4p interaction, and that interaction was abolished by truncation of 50 more amino acids from the C-terminus. Similarly, an Mpp10p fragment representing amino acids 350 to the C-terminus did interact with Mpp10p, while an Mpp10p fragment representing amino acids 400 to the end did not. This suggests that, surprisingly, Mpp10p amino acids 350–400, which do not encompass a predicted coiled-coil domain, are necessary for Imp4 interaction.

A similar analysis was carried out on the sequences in Imp4p necessary for interaction with Mpp10p (Fig. 2B). The predicted secondary structure of Imp4p contains a single N-terminal coiled-coil domain and a C-terminal domain, which contains an RNA binding motif (4). Neither the Imp4p bearing only the predicted coiled-coil domain (amino acids 1–50) nor the Imp4p minus the predicted coiled-coil domain (amino acids 50 to C-terminus) interacted with Mpp10p in the two-hybrid assay. Thus, neither domain of Imp4p alone is sufficient for Mpp10p interaction.

We used a genetic approach to probe the function of the Imp4p–Mpp10p interaction *in vivo* in the context of the normal cellular function of these two proteins. In order to study the effect of the lack of Mpp10–Imp4 protein interaction

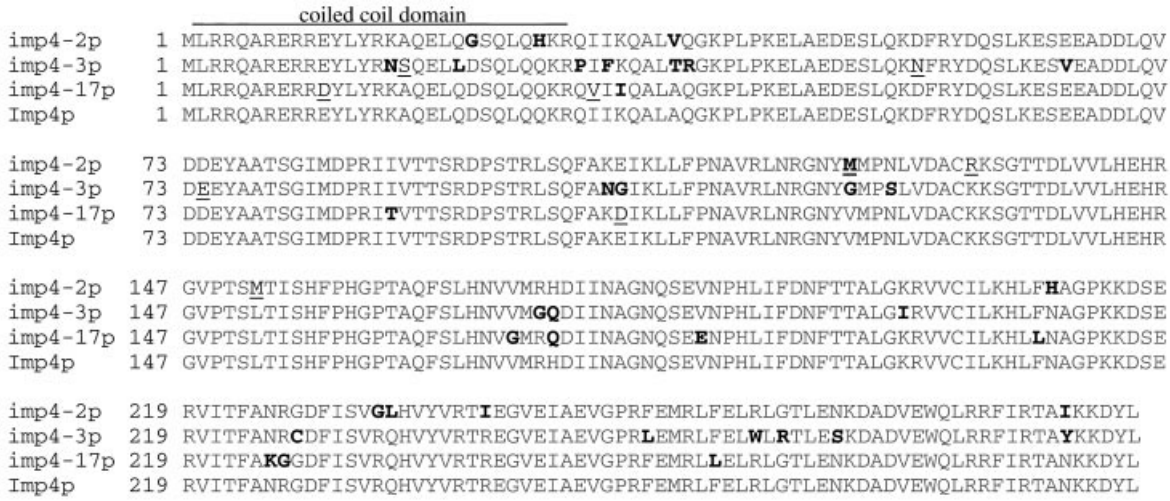

Proteins	Conditional growth	Conservative Mutations (underlined)	Non-conservative Mutations (bold)	Total Mutations
imp4-2p	ts	2	9	11
imp4-3p	cs/ ts	3	20	23
imp4-17p	ts	3	9	12

Figure 4. Mutations in the interaction-defective Imp4 proteins. The genes encoding mutated Imp4 proteins (Imp4-2p, Imp4-3p and Imp4-17p) were sequenced in both directions. Conservative mutations are indicated by an underline and non-conservative mutations are in bold. A tally of conservative and non-conservative mutations is shown for each protein in the table below.

on cell growth and ribosome biogenesis, we generated mutations in Imp4p that cause a conditional defect in Mpp10p association. We used the two-hybrid system to generate the Mpp10p interaction-defective Imp4 proteins, and then verified that they functioned in yeast and maintained their ability to confer conditional growth (Fig. 3).

The two-hybrid strain, pJ69-4A, was transformed with pACT-2-*MPP10*, which expresses Mpp10p fused to the DNA activation domain (prey plasmid). Mutant *imp4* alleles were generated by mutagenic PCR with primers containing vector sequences. Co-transformation with a gapped pAS2-1 (bait) plasmid facilitated gap repair and creation of a library of mutated *imp4* genes fused to the DNA binding domain. Transformants were selected that had both plasmids and that demonstrated Mpp10p–Imp4p interaction at 30°C by activation of the histidine reporter gene (Fig. 3). Of the 2680 colonies that grew on the triple selective medium (SD-Leu, Trp, His), 500 were patched onto three plates of the same medium to assay conditional growth at different temperatures. Transformants were incubated at 30 (permissive), 17 and 37°C (non-permissive) to test for conditional Mpp10p–Imp4p interaction-defective association. Nineteen candidate transformants that grew at 30°C but not at 17 or 37°C demonstrated mutated Imp4p interaction with Mpp10p at 30°C but not at the non-permissive temperatures (Table 1), and were re-streaked to confirm conditional growth. pAS2-1-*imp4* plasmid DNA was isolated by passage through *E.coli* JA300 and re-transformed into pJ69-4A bearing pACT-2-*MPP10*. Following plasmid rescue and re-transformation, there were 12 pAS2-1-*imp4* plasmids that conferred conditional growth on triple selective media (Table 1).

An essential gene in yeast encodes Imp4p; therefore, to be useful for further study, the mutated Imp4 proteins must function at the permissive temperature. To test this, they were assayed for their ability to complement a null allele of *IMP4*. While eight *imp4* alleles could complement the null allele, only five of them conferred conditional growth at the non-permissive temperatures (Table 1). Interestingly, all of the mutant *imp4* alleles that conferred temperature sensitivity in the two-hybrid strain (pJ69-4A) also conferred temperature-sensitive growth when Imp4p was expressed in the context of its normal cellular function. Surprisingly, one allele, *imp4-3*, also conferred cold-sensitive growth when the mutated Imp4p was expressed in the context of its normal cellular function but not in the two-hybrid strain. DNA sequencing of the five pAS2-1-*imp4* plasmids revealed that they represented three unique sequences (Fig. 4). The total number of mutations in each sequence varied between 11 and 23.

Our screen for Mpp10p interaction-defective Imp4 proteins therefore yielded three different mutated Imp4 proteins. They were isolated because (i) they were conditionally Mpp10p-interaction defective in the two-hybrid system and (ii) they conferred normal growth at the permissive temperature in the context of their normal cellular function, but slow growth at the non-permissive temperatures. Using co-immunoprecipitation, we tested the mutated Imp4ps for conditional Mpp10p interaction in the context of their normal cellular function (Fig. 5A). Anti-Imp4p antibodies were used to immunoprecipitate the mutated Imp4ps from the yeast strains grown at the designated temperatures. Mpp10p association was analyzed by western blotting with anti-Mpp10p antibodies. Surprisingly, in contrast to the two-hybrid results, the

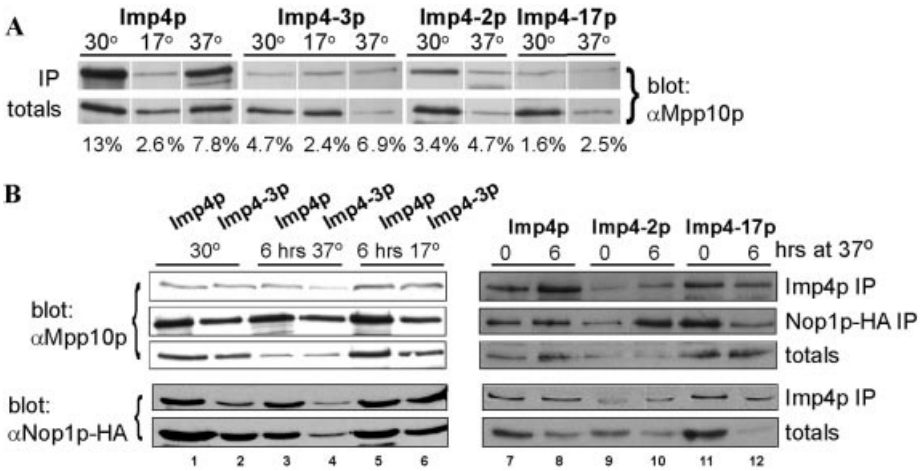

Figure 5. (**A**) The mutated Imp4ps are not Mpp10 interaction defective in the context of the SSU processome. Immunoprecipitations of wild-type Imp4p and mutated Imp4ps were carried out with guinea pig polyclonal anti-Imp4 antibody on extracts from cells grown at the indicated temperatures after 6 h of growth. The resulting protein was analyzed by western blot with rabbit anti-Mpp10 antibodies. The amount of protein run in the totals lanes represents 5% of the input used for each co-immunoprecipitation. The percent of total Mpp10p co-immunoprecipitated by the anti-Imp4 antibody was quantified and is indicated. The integrated density values (IDV, from the Alpha Innotech Imager software program) from the immunoprecipation lanes were divided by the IDV from totals lanes, which were adjusted to 100% of input: IDV_{IP} / (IDV_{total} × 20). (**B**) The integrity of the SSU processome is maintained in the presence of the mutant Imp4ps. Co-immunoprecipitations with anti-Imp4 and anti-HA antibodies were carried out on extracts from yeast where Nop1p was triple HA tagged. Cells were grown at 30°C and then shifted to 17 or 37°C for 6 h. Western blots were analyzed with anti-Mpp10p and anti-HA antibodies.

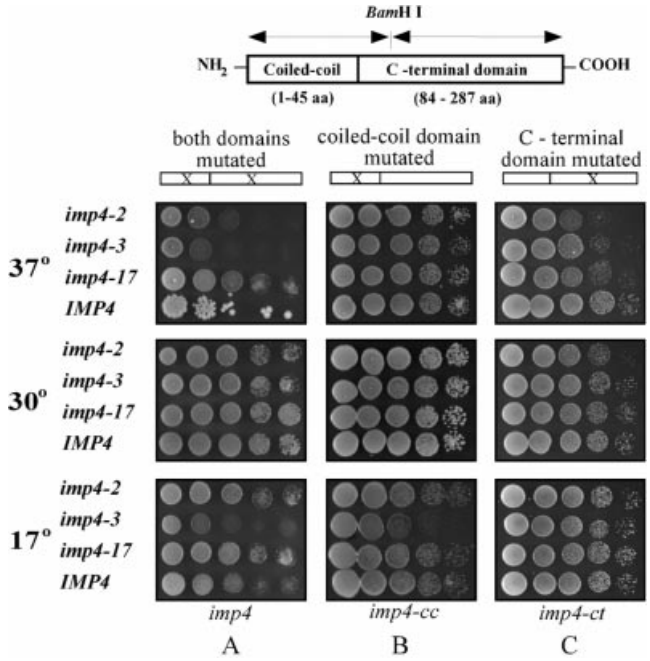

Figure 6. Mutations in Imp4p confer growth defects at 17 and 37°C. Serial dilutions of yeast expressing Imp4 proteins from the p415GPD plasmid in strains where the endogenous *IMP4* has been disrupted. (**A**) Strains bearing the plasmids with cloned *imp4-2*, *imp4-3*, and *imp4-17*. (**B**) Strains bearing plasmids that express mutated Imp4 proteins where the mutated N-terminal coiled-coil (cc) domain has been swapped onto an unmutated Imp4p C-terminal (ct) domain. (**C**) Strains bearing plasmids that express mutated Imp4 proteins where the mutated C-terminal (ct) domain has been swapped onto an unmutated coiled-coil (cc) domain.

interactions between the mutated Imp4ps and Mpp10p were not affected at the non-permissive temperatures. Because both Imp4p and Mpp10p are components of an approximately 80S RNP, which we have termed the SSU processome (3), other protein–protein interactions may remain unaffected at the non-permissive temperatures. These interactions may continue to tether Mpp10p and Imp4p to the SSU processome and hence to each other. However, since the mutated Imp4ps do confer growth defects, the mutations are affecting an essential aspect of Imp4p function.

The integrity of the SSU processome containing the mutated Imp4 proteins was assessed by co-immunoprecipitation of SSU processome components. Previously, we have shown that depletion of the U3 snoRNA or individual protein components leads to the loss of the SSU processome, visualized as the terminal knobs on nascent rRNAs (3). Nop1p, a common box C/D protein that is required for U3 snoRNA stability, was triple HA tagged by integration in the chromosomal locus. A series of co-immunoprecipitations was carried out to examine the ability of mutated Imp4p and Nop1p-HA to associate with Mpp10p, mutated Imp4p and Nop1p-HA at the permissive and non-permissive temperatures. The results indicate that there was largely no change in SSU processome integrity at the non-permissive temperatures, as the levels of co-immunoprecipitating proteins were very similar (Fig. 5B). While there appeared to be a reduction in the amount of Nop1p-HA associating with Imp4-2p, Imp4-3p and Imp4-17p at 37°C, this correlated with a decrease in the total levels of Nop1p-HA at the elevated temperature (Fig. 5B, lanes 4, 10 and 12).

In light of the multiple mutations found in each of the mutated Imp4ps, we determined whether mutations in a particular domain of Imp4p were responsible for the cold and temperature sensitivity. We divided Imp4p according to its two domains, as introduced in the results to Figure 2B: the N-terminal coiled-coil domain (cc) and the C-terminal domain (ct). Using a BamHI restriction site within the coding region of *IMP4*, sections of the mutagenized sequence were swapped with wild-type sequence to pinpoint mutations that cause the cs and ts phenotypes (Fig. 6). We compared their growth at 17,

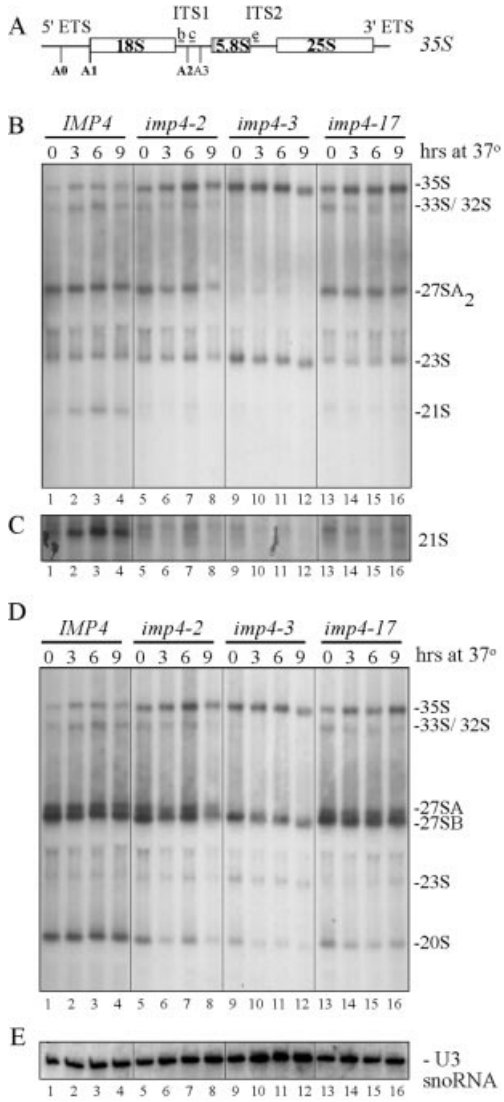

Figure 7. Mutations in Imp4p cause defects in pre-rRNA processing at 37°C. RNA was harvested at the indicated time points after the shift to 37°C from strains *imp4-2*, *imp4-3* and *imp4-17*. The RNA was analyzed for pre-rRNA precursors and for the U3 snoRNA by northern blotting. (**A**) Schematic of the organization of the nascent pre-rRNA transcript. Small letters indicate the placement of the oligonucleotide probes used to detect the precursors. (**B**) Hybridization with oligo c to detect the 35S, 33S/32S, $27SA_2$ and 23A pre-rRNAs. (**C**) A darker exposure of part of (B) to highlight the heterogeneous pre-rRNA species labeled 21S. (**D**) Hybridization with oligos b and e to detect the 35S, 33/32S, 27SA, 27SB, 23S and 20S pre-rRNAs. (**E**) Hybridization with an oligonucleotide complementary to the U3 snoRNA.

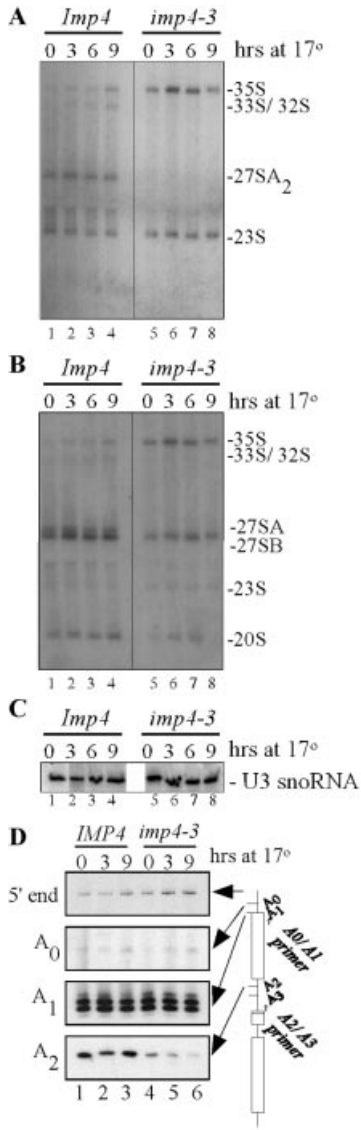

Figure 8. Mutations in Imp4p cause defects in pre-rRNA processing at 17°C. RNA was harvested at the indicated time points after the shift to 17°C from the *IMP4* and *imp4-3* strains. The RNA was analyzed for pre-rRNA precursors and for the U3 snoRNA by northern blotting. Refer to Figure 7 for the placement of the oligonucleotide probes and the legend to Figure 7 for the detectable pre-rRNAs. (**A**) Hybridization with oligo c. (**B**) Hybridization with oligos b and e. (**C**) Hybridization with an oligonucleotide complementary to the U3 snoRNA. (**D**) Primer extension analysis of RNA from yeast strain *IMP4* or *imp4-3* with the indicated oligonucleotides complementary to the pre-rRNA.

30 and 37°C by serial dilution. Generally, mutations in the C-terminus of *imp4* (*imp4p-ct)* conferred temperature sensitivity, while mutations in the N-terminus of *imp4-3* conferred cold sensitivity (*imp4-3cc*). Interestingly, the greater the number of mutations in the N-terminus, the less likely was the existence of the predicted coiled-coil domain as calculated by the COILS algorithm (data not shown). The Imp4-3cc protein, which was the only protein of the three to have no predicted coiled-coil domain, was also the only one that conferred a growth defect at 17°C. In contrast, the *imp4-2cc* and *imp4-17cc* strains, which had predicted intact N-terminal coiled-coil domains in their Imp4 proteins, were not conditional at any temperature tested. The differences in conditional sensitivities conferred by the two Imp4p domains could be indicative of their different functions. However, there is also synergy between them because the full-length mutated proteins (*imp4*) had more pronounced growth defects than either domain alone mutated (*imp4p-cc* and *imp4p-ct*; compare Fig. 6A and B with C).

We reasoned that the mutations in Imp4p would cause defects in pre-rRNA processing because they caused conditional growth defects. To investigate this, we analyzed the steady-state levels of pre-rRNAs by northern blotting with

labeled oligonucleotides specific to pre-rRNA sequences (oligos b, c and e in Fig. 7A). We studied the temperature-sensitive strains with mutated Imp4p throughout their entire length at 37°C (*imp4-2*, *imp4-3* and *imp4-17*), and the *imp4-3* strain at 17°C. The growth rate changes after 6 h at the restrictive temperature so RNA was analyzed from yeast 0, 3, 6 and 9 h after the temperature shift.

The pre-rRNA processing defects observed at 37°C in the *imp4-2* and *imp4-17* strains were similar. Probing with oligonucleotide c (Fig. 7A, lanes 1–8 and 13–16) indicated a slight increase in the levels of the nascent 35S precursor and a decrease in the levels of the precursor that extends from A_1 to A_3 (marked with a 21S; Fig. 7B and C, lanes 5–8 and 13–16). The 21S precursor is more prevalent in certain strains and has been previously described in our laboratory and others (sometimes referred to as *) (21,22). Because the normal levels of the $27SA_2$ and 27SB precursors (Fig. 7D) indicate that cleavage at A_2 and A_3 are unaffected, it is likely that a decrease in the levels of this precursor results from defective cleavage at site A_1 (see Fig. 1 for pre-rRNA processing diagram). Primer extensions to confirm this were uninformative because they cannot distinguish between the 5′ end of this precursor and the 5′ end of the mature 18S rRNA, which is much more abundant than the precursors (data not shown). Likewise, the presence of the 33S precursor indicated that cleavage at the A_0 site is intact. The 21S precursor (A_1 to A_3) appears heterogeneous from strains expressing mutant Imp4p even at 0 h (Fig. 7C, lanes 5–8 and 13–16), also indicating a defect in cleavage at A_1. Probing with oligonucleotides b and e indicated a decrease in the levels of the 20S precursor (Fig. 7D), which can also result from lack of cleavage at A_1. Figure 7E indicates that the lanes were approximately evenly loaded with RNA. In summary, taken together, these results indicate that the temperature-sensitive mutations in *imp4-2* and *imp4-17* primarily cause a defect in cleavage at A_1.

In contrast, analysis of the pre-rRNAs in the *imp4-3* strain at 37 and 17°C showed defects in cleavage at all three SSU processome-dependent sites, A_0, A_1 and A_2. The levels of the 33S and $27SA_2$ precursors were decreased, indicating a defect in cleavage at A_0 and A_2 at 37 and 17°C, respectively (Figs 7B and D, lanes 9–12; 8A and B, lanes 5–8). Similarly, at 37°C, the levels of the 23S precursor rRNA was slightly increased, consistent with defective cleavage at A_0, A_1 and A_2. A reduction in the levels of the 20S precursor was also observed at both temperatures. Figures 7D and 8C indicate that the lanes were evenly loaded with RNA, and that U3 snoRNA levels were constant at the non-permissive temperatures.

To further map the defective cleavage sites in yeast expressing mutated Imp4-3p at 17°C, primer extension analysis of RNA was carried out. The results demonstrated a clear decrease in pre-rRNA transcripts cleaved at the A_2 site (Fig. 8D, lanes 4–6). There was also a slight increase in the signal marking the 5′ of the pre-rRNA, as was expected because the levels of the 23S and 35S pre-rRNAs were detectably increased by northern blots (Fig. 8A and B). There was no change in the signal marking A_0 or A_1 cleavage in yeast expressing mutated Imp4-3p. However, primer extension to examine A_1 cleavage in precursors also examines the mature 5′ end of the 18 rRNA. Therefore, changes in cleavage at this site in pre-rRNAs may be masked by the presence of mature 18S rRNAs that are still extant after the temperature shift. The results of both the northern blots and primer extensions thus indicate that the yeast expressing mutated Imp4-3p have cleavage defects at A_0, A_1 and A_2; however, at 17°C the cleavage defect at A_2 is most pronounced.

We also investigated the pre-rRNA processing defects in the *imp4-3cc* and *imp4p-3ct* strains (Fig. 6) at their respective non-permissive temperatures (17 and 37°C). We found that the pre-rRNA processing defects in the *imp4-cc* strain mimic those found in the parent *imp4-3* strain (Fig. 8), with pronounced cleavage defects at A_0, A_1 and A_2 (data not shown). In contrast, the pre-rRNA processing defects in the *imp4p-3ct* strain mimic those found in the *imp4-2* and *imp4-17* strains (data not shown). Therefore, mutations that affect growth in the N-terminal coiled-coil domain of Imp4p cause different pre-rRNA processing defects than those in the C-terminus.

DISCUSSION

The SSU processome is a large RNP with multiple protein–protein interactions. We investigated the function of one pair of SSU processome protein–protein interactions, Mpp10p–Imp4p. Amino acids 350–400 in Mpp10p were essential for Imp4p interaction as determined by two-hybrid analysis while neither of the two tested truncations of Imp4p were sufficient for Mpp10p interaction. To further explore the nature of the Mpp10p–Imp4p interaction, we used a reverse two-hybrid system approach to generate Imp4 proteins that were conditionally defective for interaction with Mpp10p by two-hybrid analysis, and then studied their function in the context of the SSU processome. Surprisingly, none of the mutations affected Mpp10p–Imp4p interaction at the non-permissive temperatures in the context of their normal cellular function. However, both growth and pre-rRNA processing were impaired at the non-permissive temperatures, indicating defects in Imp4p function. All three mutated Imp4ps caused temperature sensitivity; one of them also caused cold sensitivity. Domain swapping revealed that the cold sensitivity was imparted by mutations in the N-terminal coiled-coil domain, while mutations in the C-terminal portion conferred temperature sensitivity. The two mutated Imp4 proteins that conferred temperature sensitivity resulted in pre-rRNA processing defects primarily at site A_1, while the mutated Imp4p that conferred both temperature and cold sensitivity resulted in pre-rRNA processing defects at all of the SSU processome-dependent sites, A_0, A_1 and A_2, with a more pronounced defect at A_2.

It is interesting that one mutated Imp4p (Imp4-3p) conferred only temperature sensitivity in the two-hybrid strain but both temperature and cold sensitivity in the context of the SSU processome. Cold-sensitive mutations are hallmarks of defects in macromolecular assembly (23), suggesting that the SSU processome is inefficiently or slowly formed in the presence of this mutated Imp4p. Further support for this comes from the observation that the mutations that confer cold sensitivity occur in the coiled-coil domain, a known protein–protein interaction domain, likely interfering with its predicted function in protein binding.

Reverse two-hybrid screens to generate interaction-defective proteins have been used to examine viral protein interactions (24), to examine interaction of non-essential

yeast proteins (25) and to map interacting protein domains (26). This approach has not previously been used as we have used it here: to study the function of the interaction of two essential proteins. To be successful, the conditionally interaction-defective proteins generated in the two-hybrid strain must complement their null alleles at the permissive temperature, indicating full function. They must also continue to confer conditional growth. Three different mutated Imp4 proteins met these criteria. However, co-immunoprecipitation experiments at the non-permissive temperatures indicated that these mutated Imp4 proteins were not defective for Mpp10p interaction. Therefore, it is likely that while the mutated Imp4p–Mpp10p proteins are interaction defective in a binary arrangement (two-hybrid strain), in the context of the SSU processome they are held in close proximity by multiple other protein and RNA interactions. Since there are many cellular multi-protein complexes (27,28), our results have implications for the study of individual protein–protein interactions *in vivo*.

The C-terminus of Imp4p contains a recently identified novel 17 amino acid RNA binding domain, the σ^{70}-like motif, which unites the Imp4 superfamily of RNA binding proteins, all of which are required for ribosome biogenesis (4). These 17 amino acids may not be the only RNA binding domain in Imp4 because the two members of the Imp4 superfamily members that were tested have persistent RNA binding ability, but altered specificity, upon deletion of this motif. Therefore, the mutations in Imp4, particularly those in the C-terminus, may also interfere with Imp4–RNA interaction. We have proposed (4) that Imp4 may contact the pre-rRNA, and therefore these mutations may interfere with Imp4p's function in pre-rRNA folding and processing.

ACKNOWLEDGEMENTS

We thank Philip James for strain pJ69-4A and Veni Manickam for technical assistance. J.E.G.G. was supported by predoctoral fellowships from the National Institutes of Health (GM20905 and GM07223). This work was supported by the National Institutes of Health grant GM52581 to S.J.B.

REFERENCES

1. Venema,J. and Tollervey,D. (1999) Ribosome synthesis in *Saccharomyces cerevisiae*. *Annu. Rev. Genet.*, **33**, 261–311.
2. Kressler,D., Linder,P. and de la Cruz,J. (1999) Protein trans-acting factors involved in ribosome biogenesis in *Saccharomyces cerevisiae*. *Mol. Cell. Biol.*, **19**, 7897–7912.
3. Dragon,F., Gallagher,J.E., Compagnone-Post,P.A., Mitchell,B.M., Porwancher,K.A., Wehner,K.A., Wormsley,S., Settlage,R.E., Shabanowitz,J., Osheim,Y. *et al*. (2002) A large nucleolar U3 ribonucleoprotein required for 18S ribosomal RNA biogenesis. *Nature*, **417**, 967–970.
4. Wehner,K.A. and Baserga,S.J. (2002) The σ^{70}-like motif: a eukaryotic RNA binding domain unique to a superfamily of proteins required for ribosome biogenesis. *Mol. Cell*, **9**, 329–339.
5. Beltrame,M., Henry,Y. and Tollervey,D. (1994) Mutational analysis of an essential binding site for the U3 snoRNA in the 5′ external transcribed spacer of yeast pre-rRNA. *Nucleic Acids Res.*, **22**, 5139–5147.
6. Beltrame,M. and Tollervey,D. (1995) Base pairing between U3 and the pre-ribosomal RNA is required for 18S rRNA synthesis. *EMBO J.*, **14**, 4350–4356.
7. Westendorf,J.M., Rao,P.N. and Gerace,L. (1994) Cloning of cDNAs for M-phase phosphoproteins recognized by the MPM2 monoclonal antibody and determination of the phosphorylated epitope. *Proc. Natl Acad. Sci. USA*, **91**, 714–718.
8. Westendorf,J.M., Konstantinov,K.N., Wormsley,S., Shu,M.D., Matsumoto-Taniura,N., Pirollet,F., Klier,F.G., Gerace,L. and Baserga,S.J. (1998) M phase phosphoprotein 10 is a human U3 small nucleolar ribonucleoprotein component. *Mol. Biol. Cell*, **9**, 437–449.
9. Dunbar,D.A., Wormsley,S., Agentis,T.M. and Baserga,S.J. (1997) Mpp10p, a U3 small nucleolar ribonucleoprotein component required for pre-18S rRNA processing in yeast. *Mol. Cell. Biol.*, **17**, 5803–5812.
10. Lee,S.J. and Baserga,S.J. (1999) Imp3p and Imp4p: two specific components of the U3 small nucleolar ribonucleoprotein that are essential for pre-18S rRNA processing. *Mol. Cell. Biol.*, **19**, 5441–5452.
11. Vidal,M., Braun,P., Chen,E., Boeke,J.D. and Harlow,E. (1996) Genetic characterization of a mammalian protein-protein interaction domain by using a yeast reverse two-hybrid system. *Proc. Natl Acad. Sci. USA*, **93**, 10321–10326.
12. James,P., Halladay,J. and Craig,E.A. (1996) Genomic libraries and a host strain designed for highly efficient two-hybrid selection in yeast. *Genetics*, **144**, 1425–1436.
13. Clarke,L. and Carbon,J. (1980) Isolation of the centromere-linked CDC10 gene by complementation in yeast. *Proc. Natl Acad. Sci. USA*, **77**, 2173–2177.
14. Muhlrad,D., Hunter,R. and Parker,R. (1992) A rapid method for localized mutagenesis of yeast genes. *Yeast*, **8**, 79–82.
15. Mumberg,D., Muller,R. and Funk,M. (1995) Yeast vectors for the controlled expression of heterologous proteins in different genetic backgrounds. *Gene*, **156**, 119–122.
16. Longtine,M.S., McKenzie,A.R., Demarini,D.J., Shah,N.G., Wach,A., Brachat,A., Philippsen,P. and Pringle,J.R. (1998) Additional modules for versatile and economical PCR-based gene deletion and modification in *Saccharomyces cerevisiae*. *Yeast*, **14**, 953–961.
17. Ausubel,F., Brent,R., Kingston,R.E., Moore,D.D., Seidman,J.G., Smith,J.A. and Struhl,K. (1995) *Short Protocols in Molecular Biology*, 3rd Edn. John Wiley and Sons, Inc.
18. Beltrame,M. and Tollervey,D. (1992) Identification and functional analysis of two U3 binding sites on yeast pre-ribosomal RNA. *EMBO J.*, **11**, 1531–1542.
19. Samarsky,D.A. and Fournier,M.J. (1998) Functional mapping of the U3 small nucleolar RNA from the yeast *Saccharomyces cerevisiae*. *Mol. Cell. Biol.*, **18**, 3431–3444.
20. Maden,B.E., Corbett,M.E., Heeney,P.A., Pugh,K. and Ajuh,P.M. (1995) Classical and novel approaches to the detection and localization of the numerous modified nucleotides in eukaryotic ribosomal RNA. *Biochimie*, **77**, 22–29.
21. Lee,S.J. and Baserga,S.J. (1997) Functional separation of pre-rRNA processing steps revealed by truncation of the U3 small nucleolar ribonucleoprotein component, Mpp10. *Proc. Natl Acad. Sci. USA*, **94**, 13536–13541.
22. Torchet,C., Jacq,C. and Hermann-Le Denmat,S. (1998) Two mutant forms of the S1/TPR-containing protein Rrp5p affect the 18S rRNA synthesis in *Saccharomyces cerevisiae*. *RNA*, **4**, 1636–1652.
23. Guthrie,C., Nashimoto,H. and Nomura,M. (1969) Structure and function of *Escherichia coli* ribosomes. VII. Cold-sensitive mutations defective in ribosome assembly. *Proc. Natl Acad. Sci. USA*, **63**, 384–391.
24. Hope,D.A., Diamond,S.E. and Kirkegaard,K. (1997) Genetic dissection of interaction between poliovirus 3D polymerase and viral protein 3AB. *J. Virol.*, **71**, 9490–9498.
25. Cayrol,C., Cabrolier,G. and Ducommun,B. (1997) Use of the two-hybrid system to identify protein-protein interaction temperature-sensitive mutants: application to the CDK2/p21Cip1 interaction. *Nucleic Acids Res.*, **25**, 3743–3744.
26. Barrett,J.G., Manning,B.D. and Snyder,M. (2000) The Kar3p kinesin-related protein forms a novel heterodimeric structure with its associated protein Cik1p. *Mol. Biol. Cell*, **11**, 2373–2385.
27. Ho,Y., Gruhler,A., Heilbut,A., Bader,G.D., Moore,L., Adams,S.L., Millar,A., Taylor,P., Bennett,K., Boutilier,K. *et al*. (2002) Systematic identification of protein complexes in *Saccharomyces cerevisiae* by mass spectrometry. *Nature*, **415**, 180–183.
28. Gavin,A.C., Bosche,M., Krause,R., Grandi,P., Marzioch,M., Bauer,A., Schultz,J., Rick,J.M., Michon,A.M., Cruciat,C.M. *et al*. (2002) Functional organization of the yeast proteome by systematic analysis of protein complexes. *Nature*, **415**, 141–147.